Journal of Catalysis **196,** 293–301 (2000)
doi:10.1006/jcat.2000.3048, available online at http://www.idealibrary.com on IDEAL®

Ionic Dispersion of Pt and Pd on CeO_2 by Combustion Method: Effect of Metal–Ceria Interaction on Catalytic Activities for NO Reduction and CO and Hydrocarbon Oxidation

Parthasarathi Bera,* K. C. Patil,† V. Jayaram,* G. N. Subbanna,‡ and M. S. Hegde*,[1]

*Solid State and Structural Chemistry Unit, Indian Institute of Science, Bangalore 560012, India; †Department of Inorganic and Physical Chemistry, Indian Institute of Science, Bangalore 560012, India; and ‡Materials Research Centre, Indian Institute of Science, Bangalore 560012, India

Received April 13, 2000; revised August 21, 2000; accepted August 28, 2000

Ceria-supported Pt and Pd catalysts have been synthesized by the combustion method. The catalysts are characterized by X-ray diffraction (XRD), transmission electron microscopy (TEM), and X-ray photoelectron spectroscopy (XPS). Pt and Pd metals are ionically dispersed on the CeO_2 surface of crystallite sizes in the range of 15–20 nm. In 1% Pt/CeO_2 Pt is found to be in the $+2$ and $+4$ oxidation states whereas Pd is in the $+2$ state in 1% Pd/CeO_2. Catalytic activities for NO reduction by CO, NH_3, CH_4, and C_3H_8 and CO, CH_4, and C_3H_8 oxidation by O_2 have been investigated over all these catalysts using the temperature-programmed reaction technique. The results are compared with Pt and Pd metals dispersed on α-Al_2O_3 support prepared by the combustion technique. Both oxidation and reduction reactions occur at much lower temperatures over M/CeO_2 compared to those over M/Al_2O_3 (M = Pt, Pd). The rate and turnover frequency of NO + CO and CO + O_2 reactions over M/CeO_2 are higher than those over M/Al_2O_3. The observed enhanced catalytic activity of M/CeO_2 has been attributed to the ionic dispersion of Pt and Pd on CeO_2 leading to a strong metal–ceria interaction in the form of solid solution, $Ce_{1-x}M_xO_{2-(4-n)x/2}$, having linkages of the type $-O^{2-}-Ce^{4+}-O^{2-}-M^{n+}-O^{2-}-$ ($n = 2$, 4) on the CeO_2 surface. © 2000 Academic Press

Key Words: **combustion synthesis; metal–ceria interaction; Pt/CeO_2; Pd/CeO_2; NO; CO; hydrocarbon.**

INTRODUCTION

In recent years, much attention has been focused on CeO_2-supported noble metal catalysts due to their applications in automotive exhausts. Noble metal catalysts supported on Al_2O_3 (1) are well-known three-way catalysts (TWC). CeO_2 is added as a promoter to TWC for its oxygen storage capacity (OSC) and stabilization of the metal dispersion (2–7). CeO_2 along with BaO is added to Al_2O_3-supported noble metal catalysts to improve its performance (8). Recently, Fernández-García *et al.* (9) have shown the influence of ceria on Pd activity for the CO + O_2 reaction. Therefore, CeO_2 seems to have a promoting effect on the metal in addition to acting as a support. Besides these investigations, several authors have reported different kinds of interaction between noble metals and ceria and their effects on catalytic activities (10–18). These studies have shown that the nature and extent of interaction depend on particular noble metal, catalyst pretreatment, preparation technique, size of CeO_2 crystallite, lattice oxygen, and so on. Despite these studies, the electronic structure of noble metals on the CeO_2 surface and the role played by CeO_2 in promoting the catalytic reactions are not well understood.

Recently, we have reported the preparation by the combustion technique of Cu/CeO_2 (19) and nanosize noble metal particles dispersed on α-Al_2O_3 (20, 21) which are active catalysts for NO reduction and CO and hydrocarbon oxidation. Here we report the synthesis of M/CeO_2 (M = Pt, Pd) catalysts by the combustion method for the first time. Interestingly, unlike α-Al_2O_3 both Pt and Pd have been found to be ionically dispersed over CeO_2 support. The objectives of the present studies are to investigate the interaction between noble metals and ceria in M/CeO_2 and its comparative effects on reactivity toward NO reduction and CO, CH_4, and C_3H_8 oxidation with M/Al_2O_3.

EXPERIMENTAL

Preparation of Catalysts

The combustion mixture for the preparation of 1% Pt/CeO_2 contained $(NH_4)_2Ce(NO_3)_6$, H_2PtCl_6, and $C_2H_6N_4O_2$ (oxalyldihydrazide) in the mole ratio 0.99 : 0.01 : 2.33. Oxalyldihydrazide (ODH) prepared from diethyl oxalate and hydrazine hydrate was used as the fuel (22). In a typical preparation, 10 g of $(NH_4)_2Ce(NO_3)_6$ (E. Merck India Ltd., 99.9%), 0.095 g of H_2PtCl_6 (Ranbaxy Laboratories Ltd., 99%), and 5.175 g of ODH were dissolved in the minimum volume of water in a borosilicate dish of 130 cm^3 capacity. The dish containing the redox mixture was introduced into a muffle furnace maintained

[1] To whom correspondence should be addressed. Fax: +91-80-3601310. E-mail: mshegde@sscu.iisc.ernet.in.

0021-9517/00 $35.00

at 350°C. Initially the solution boiled with frothing and foaming and underwent dehydration. At the point of complete dehydration, the surface ignited, burning with a flame (∼1000°C) and yielding a voluminous solid product within 5 min. Similarly, 1% Pd/CeO_2 has been prepared. In the case of Pd the precursor used was $PdCl_2$ (Glaxo India Ltd. 99%). The color of 1% Pt/CeO_2 is light gray and 1% Pd/CeO_2 is dull white. Similarly, 2–5% Pt/CeO_2 and 5% and 10% Pd/CeO_2 were also prepared by this method. Details of the preparation of α-Al_2O_3-supported metal particles have been described earlier (20). These compounds were prepared in an open muffle furnace kept in a fume cupboard with exhaust. The reaction can be controlled by carrying out the combustion in an open vessel. As-prepared combustion products without further reduction by H_2 are used for all the studies including the catalytic reactions.

Characterization of Catalysts

XRD patterns of the catalysts were recorded on a Siemens D5005 diffractometer using Cu$K\alpha$ radiation with a scan rate of 2° min^{-1}. A JEOL JEM-200CX transmission electron microscope operated at 200 kV was used to carry out TEM studies. Samples for TEM studies were prepared by taking a small quantity of powder in ethanol/acetone medium and was ultrasonicated for a few minutes. The resultant slurry was then deposited on a holey carbon-coated 200 mesh copper grid. Suitable regions in the grid were selected for electron diffraction and microscopy.

XPS of these materials were recorded in an ESCA-3 Mark II spectrometer (VG Scientific Ltd., England) using Al$K\alpha$ radiation (1486.6 eV). Binding energies were calculated with respect to C(1*s*) at 285 eV. Binding energies were measured with a precision of ±0.2 eV. For XPS analysis the powder samples were made into pellets of 8 mm diameter and placed into an ultrahigh-vacuum (UHV) chamber at 10^{-9} Torr housing the analyzer. Prior to mounting the sample into the analyzing chamber it was kept in the preparation chamber at 10^{-9} Torr for 5 h in order to desorb any volatile species present on the sample.

Adsorption Studies

Adsorption of CO on 1% Pt/CeO_2 and 1% Pt/Al_2O_3 was carried out in a constant volume glass system. Typically 0.5 g of the catalyst was degassed at 250°C in a vacuum system (10^{-6} Torr) for 3 h, and then cooled to 0°C. A known volume of CO was passed into the sample tube and the pressure was measured by a digital pirani gauge calibrated against N_2. The volume of CO adsorbed expressed in cubic centimeters (STP) was accurate within ±10%.

Temperature-Programmed Reaction (TPR)

The catalytic reactions were carried out in a temperature-programmed reaction system equipped with a quadrupole mass spectrometer QXK300 (VG Scientific Ltd., England) for product analysis in a packed-bed tubular reactor. The details of this home-made TPR set-up have been described elsewhere (23). Typically 0.1–0.2 g of the catalyst was loaded in a quartz tube reactor of 20 cm length and 6 mm diameter. The reactor can be heated from 30 to 750°C at a rate of 15°C min^{-1} and the sample temperature was measured by a fine chromel–alumel thermocouple immersed in the catalyst. The quartz tube was evacuated to 10^{-6} Torr. The gaseous products were sampled through a fine control leak valve to an ultrahigh-vacuum (UHV) system housing the quadrupole mass spectrometer at 10^{-9} Torr. The gases were passed over the catalyst at a flow rate of 25 μmol s^{-1} and the flow rate can be varied from 10–40 μmol s^{-1}. Accordingly, space velocity was in the range of 5.0×10^{-5} to 2.0×10^{-4} mol g^{-1} s^{-1}. The dynamic pressure of gases was in the range of 1 to 20 Torr in the reaction system in all of the experiments. All the masses were scanned every 10 s. At the end of the reaction, the intensity of each mass as a function of temperature (thermogram) was generated. NO, NH_3, CO, CH_4, C_3H_8, and O_2 gases were obtained from Bhoruka Gases Ltd., Bangalore. Their purities were better than 99% as analyzed by the quadrupole mass spectrometer.

RESULTS

Structural Studies

XRD patterns of 1–3% Pt/CeO_2 are shown in Fig. 1. The patterns can be indexed for CeO_2 with fluorite structure. The diffraction lines are broad and the crystallite sizes calculated by using the Debye–Scherrer method are in the range of 15–25 nm. Diffraction lines due to Pt metal or any platinum oxides have not been seen. Even the XRD pattern of as-prepared 5% Pt/CeO_2 does not contain Pt metal peaks. The 1–5% Pt/CeO_2 samples when heated in air at 500°C for 40 h do not show any Pt metal or oxide peaks. However, on heating at 800°C for 40 h, 2–5% Pt/CeO_2 samples show Pt metal peaks in the XRD patterns where Pt peak intensity increases as the concentration of Pt increases. XRD patterns of 1%, 5%, and 10% Pd/CeO_2 are given in Fig. 2. Here also Pd metal or PdO peaks are not observed in the as-prepared samples. Crystallites of CeO_2 calculated from the XRD pattern are in the range of 20 nm. Pd metal or PdO could not be detected on heating of 1% and 5% Pd/CeO_2 catalysts at 800°C for 24 h. However, 10% Pd/CeO_2 sample shows weak diffraction lines due to PdO on heating at 800°C for 24 h. Thus, 1% Pt/CeO_2 and 1%, 5%, and 10% Pd/CeO_2 samples are devoid of Pt or Pd metal particles or their oxides in the as-prepared as well as heated samples. Catalytic studies are therefore carried out using 1% Pt/CeO_2 and 1% Pd/CeO_2 catalysts.

TEM of the 1% M/CeO_2 shows that the crystallite sizes are in the range of 15–20 nm which agrees well with the

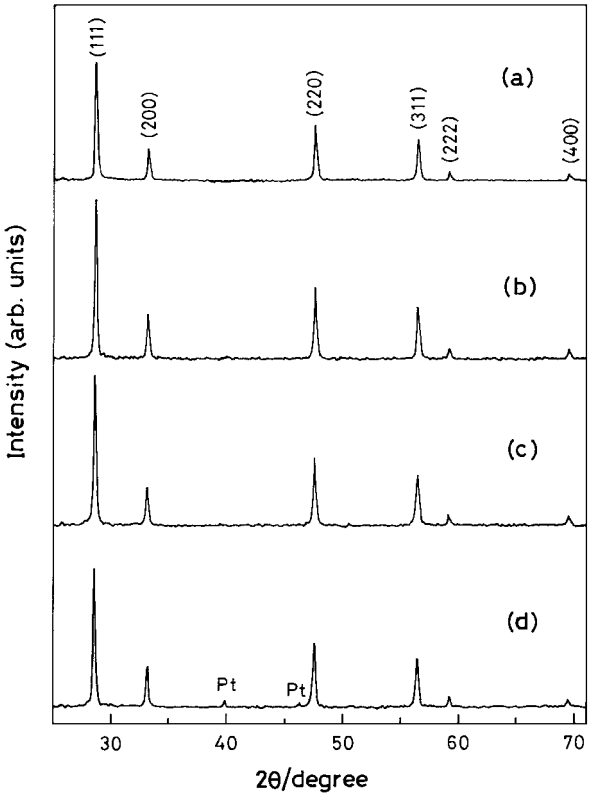

FIG. 1. XRD patterns of as-prepared (a) 1% Pt/CeO_2, (b) 2% Pt/CeO_2, and (c) 3% Pt/CeO_2 catalysts and (d) 3% Pt/CeO_2 catalyst after heating at 800°C for 40 h.

XRD measurements. Typical TEM images of 1% M/CeO_2 are given in Fig. 3. The polycrystalline diffraction pattern observed could be indexed only to CeO_2 with fluorite structure. The morphology of CeO_2 crystallites is cubic. Pt or Pd metal diffraction rings are completely absent in the pattern. Even high-resolution images of as-prepared 4% Pt/CeO_2 give lattice fringes corresponding to (111) and (100) planes of CeO_2. However, 2–5% Pt/CeO_2 samples heated at 800°C for 40 h reveal the presence of Pt particles of 2–4 nm in the image and a ring is observed due to Pt metal in the electron diffraction. In contrast to Pt and Pd on CeO_2, nanosize metal particles dispersed on α-Al_2O_3 can be seen. TEM images of 1% Pt/Al_2O_3 and 1% Pd/Al_2O_3 are given in Figs. 3c and 3d for comparison and the average sizes of Pt and Pd particles are 7 and 10 nm, respectively. TEM results confirm that the metal particles are not present in the as-prepared 1% M/CeO_2 catalysts.

XPS Studies

Photoelectron spectra of the Pt(4*f*) core level region of Pt metal and 1%, 3%, and 4% Pt/CeO_2 are given in Fig. 4. In the Pt metal, $4f_{7/2,5/2}$ peaks are observed at 71.0 and 74.3 eV respectively. The Pt(4*f*) region shows peaks due to multiple oxidation states in the Pt/CeO_2 catalysts. The Pt($4f_{7/2,5/2}$) peaks in Pt/CeO_2 catalysts were resolved into sets of spin orbital doublets. Accordingly, Pt(4*f*) peaks at 71.7 and 74.9 eV and 74.0 and 77.2 eV in 1%, 3%, and 4% Pt/CeO_2 can be assigned to Pt^{2+} and Pt^{4+} oxidation states (12, 24). Peaks due to Pt(4*f*) metal at 71.0 and 74.2 eV are not observed in as-prepared 1–5% Pt/CeO_2 catalysts. Thus, Pt metal in 1–5% Pt/CeO_2 is in the +2 and +4 oxidation states. However, 2–5% samples when heated to 800°C for 40 h do show Pt(4*f*) peaks due to Pt^0, Pt^{2+}, and Pt^{4+}. The Pt(4*f*) region could be resolved into three sets of spin orbit peaks and indeed Pt^0 ($4f_{7/2,5/2}$) peaks at 71.0 and 74.2 eV were seen. The intensity of the Pt^0 peak is about 25% of the total Pt(4*f*) envelope in the 2% Pt/CeO_2 heated sample. Pd(3*d*) spectra are given in Fig. 5 for 1% Pd/CeO_2, 5% Pd/CeO_2, 10% Pd/CeO_2, and 1% Pd/Al_2O_3. Pd($3d_{5/2,3/2}$) peaks observed at 338.0 and 342.8 eV in Pd/CeO_2 catalysts are shifted by 2 eV with respect to Pd metal in 1% Pd/Al_2O_3. Binding energies of Pd(3*d*) peaks in Pd/CeO_2 catalysts agree well with those of Pd^{2+} in $PdCl_2$ indicating that Pd is in the +2 state (25). Thus, the shifted Pd^{2+} peaks show that Pd on CeO_2 is in the highly ionic state. Even in 10% Pd/CeO_2, Pd metal peaks are not seen. This observation agrees well with the XRD and TEM results. In Fig. 6 Ce(3*d*) peaks obtained from 1% Pt/CeO_2 and 1% Pd/CeO_2 are shown. The spectra with satellite features (marked in the figure) correspond to CeO_2 with Ce in the +4 oxidation state (12, 26).

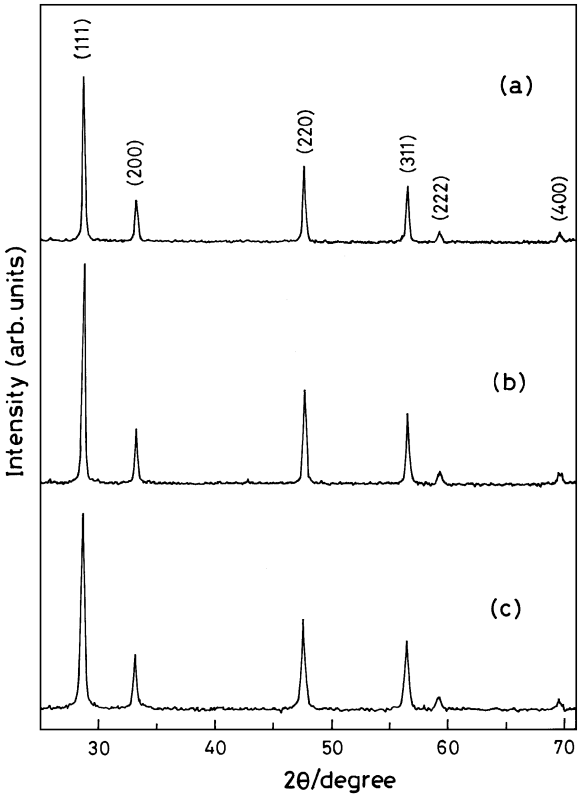

FIG. 2. XRD patterns of as-prepared (a) 1% Pd/CeO_2, (b) 5% Pd/CeO_2, and (c) 10% Pd/CeO_2 catalysts.

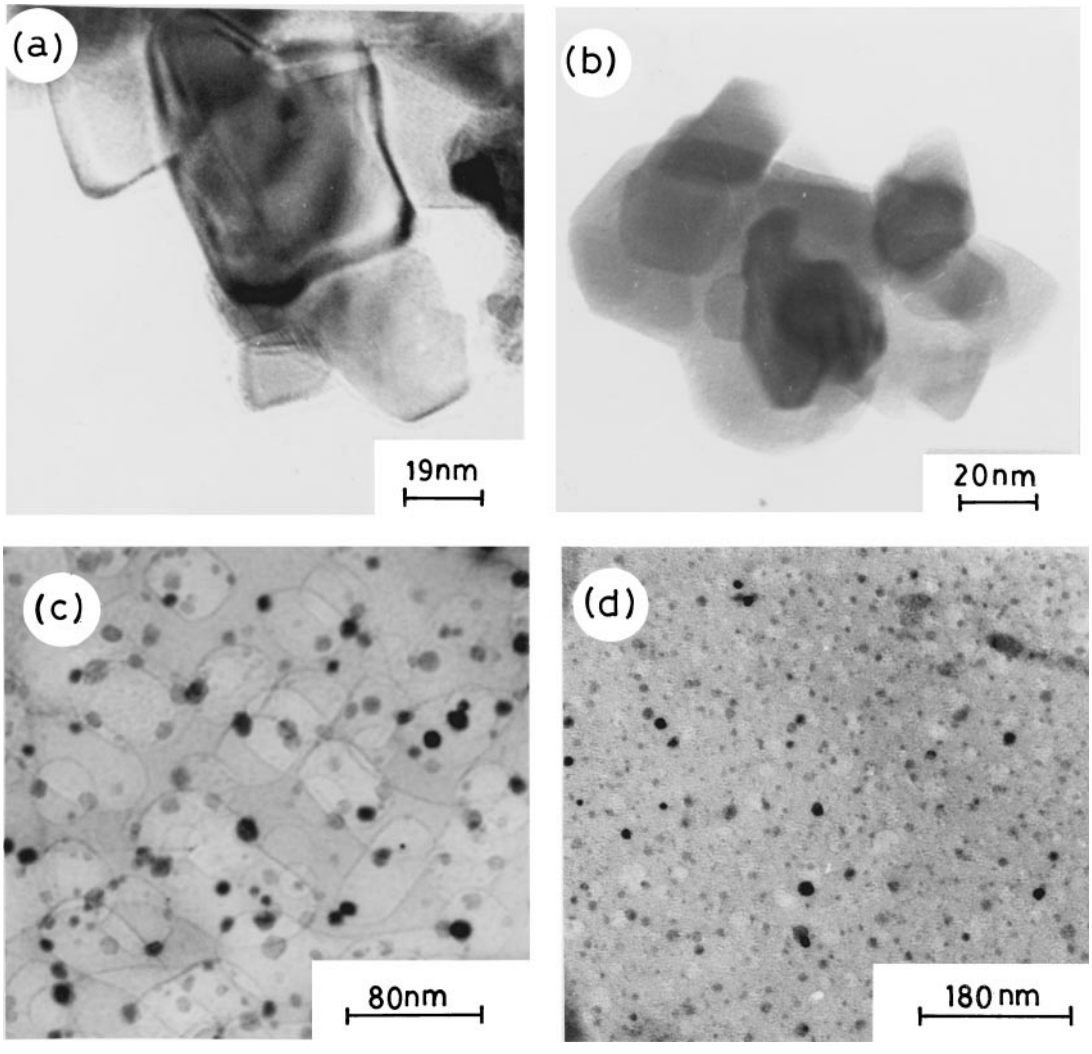

FIG. 3. TEM of (a) 1% Pt/CeO_2, (b) 1% Pd/CeO_2, (c) 1% Pt/Al_2O_3, and (d) 1% Pd/Al_2O_3.

Surface concentrations of metal ions in M/CeO_2 have been estimated by the relation

$$\frac{X_M}{X_{Ce}} = \frac{I_M}{I_{Ce}} \frac{\sigma_{Ce}\lambda_{Ce}D_E(Ce)}{\sigma_M\lambda_M D_E(M)}, \quad [1]$$

where X, I, σ, λ, and D_E are the surface concentration, intensity, photoionization cross section, mean escape depth, and geometric factors, respectively. Integrated intensities of Pt(4*f*), Pd(3*d*), and Ce(3*d*) peaks have been taken into account to estimate the concentration. Photoionization cross section and mean escape depths have been obtained from Scofield (27) and Penn (28), respectively. The surface concentration of Pt is 15% in 1% Pt/CeO_2 whereas it is 5% in 1% Pd/CeO_2.

Adsorption Studies

The adsorption isotherm of CO over 1% Pt/CeO_2 at 0°C is given in Fig. 7. In the same figure, the CO adsorption isotherm on 1% Pt/Al_2O_3 is also shown for comparison. This experiment was carried out to examine the dispersion of Pt on CeO_2 and Al_2O_3. The isotherms follow Langmuir type of adsorption. Saturation CO adsorption is 0.15 $cm^3 g^{-1}$ for 1% Pt/CeO_2 and it is 3 times more than that on 1% Pt/Al_2O_3. Translating these data into the number of CO molecules adsorbed per Pt atom gives 0.11 and 0.012 CO molecules in 1% Pt/CeO_2 and 1% Pt/Al_2O_3, respectively. Nearly an order of magnitude increase in CO adsorption over Pt/CeO_2 with respect to Pt/Al_2O_3 can be rationalized from fine Pt metal particles (7 nm) dispersed on Al_2O_3 compared to Pt ions on CeO_2. The total number of surface Pt atoms was calculated by taking (111) and (100) faces of Pt in 7-nm Pt clusters. The ratio of the number of CO molecules to the number of Pt surface atoms is 0.13. Therefore, the sticking coefficient of CO on Pt/Al_2O_3 observed here is 0.13 which agrees well with the value reported by Gruber (29).

Assuming Pt taken in 1% Pt/CeO_2 is dispersed as ions on 15-nm surfaces of CeO_2 crystallites and Ce^{4+} ions are

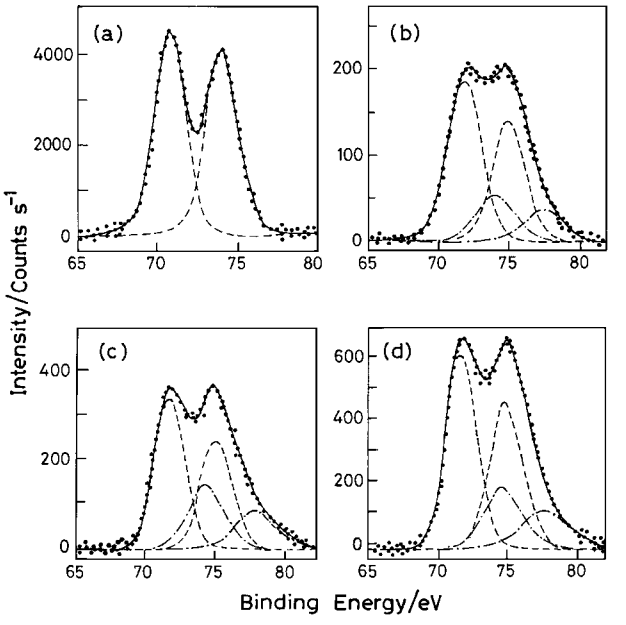

FIG. 4. XPS of Pt(4*f*) core level region of (a) Pt metal foil, (b) 1% Pt/CeO_2, (c) 3% Pt/CeO_2, and (d) 4% Pt/CeO_2.

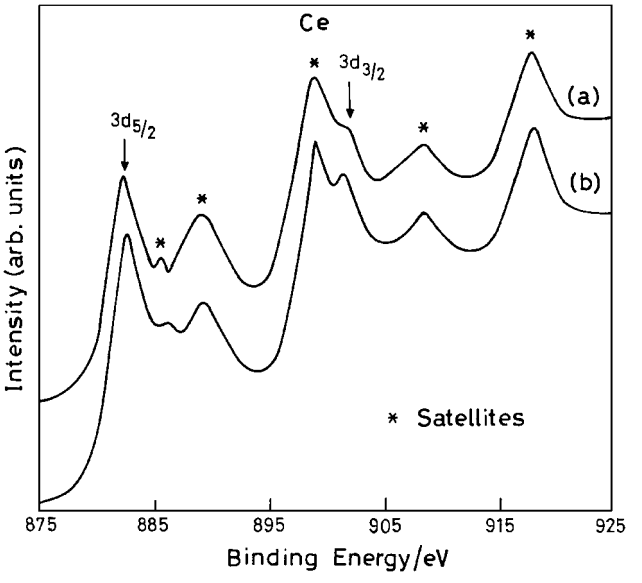

FIG. 6. XPS of Ce(3*d*) core level region of (a) 1% Pt/CeO_2 and (b) 1% Pd/CeO_2.

replaced by Pt^{2+} or Pt^{4+} ions, 20% of Ce^{4+} ions can be replaced by Pt^{2+} or Pt^{4+} ions. Further, the ratio of the number of CO molecules to the number of Pt ions on 1% Pt/CeO_2 is 0.12. Thus, the sticking coefficients of CO on 1% Pt/CeO_2 and 1% Pt/Al_2O_3 are in the same range. Nearly 10 times increase in CO adsorption on 1% Pt/CeO_2 compared to 1% Pt/Al_2O_3 is therefore primarily due to a higher dispersion of Pt ions on CeO_2. On the other hand, pure CeO_2 and Al_2O_3 do not show CO adsorption at 0°C.

Temperature-Programmed Reaction (TPR)

NO reduction by CO, NH_3, CH_4, and C_3H_8 and CO, CH_4, and C_3H_8 oxidation by O_2 have been carried out over 1% Pt/CeO_2 and 1% Pd/CeO_2 catalysts.

NO reduction by CO. An equimolar mixture of NO and CO passed over these catalysts shows N_2 and CO_2 formation. A sharp decrease in NO concentration occurs at 140°C and below 175°C complete conversion of NO has been observed. An increase in CO_2 ($m/z = 44$) concentration with a simultaneous decrease in NO ($m/z = 30$) concentration is taken as the measure of NO conversion. Since N_2 and CO

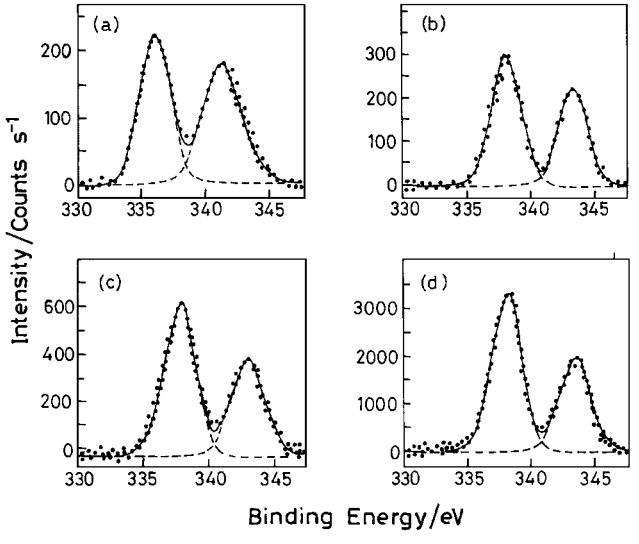

FIG. 5. XPS of Pd(3*d*) core level region of (a) 1% Pd/Al_2O_3, (b) 1% Pd/CeO_2, (c) 5% Pd/CeO_2, and (d) 10% Pd/CeO_2.

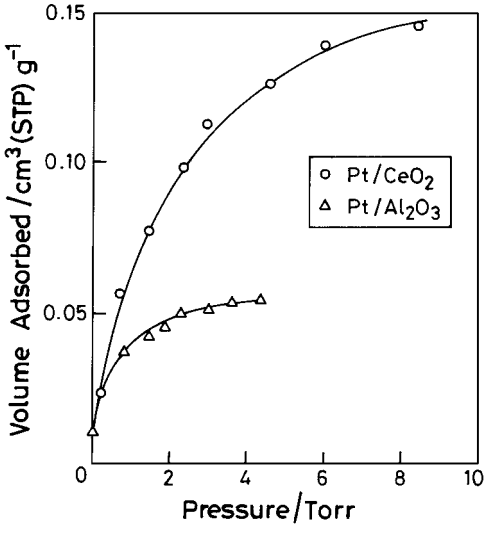

FIG. 7. Adsorption isotherms of CO on 1% Pt/CeO_2 and 1% Pt/Al_2O_3 at 0°C.

have the same mass, above 175°C $m/z = 28$ is due to N_2. Similarly, total conversion of NO is observed below 270°C on 1% Pt/CeO_2. The reaction can be written as

$$2NO + 2CO \rightarrow N_2 + 2CO_2. \quad [2]$$

NO reduction by NH_3. NO reduction by NH_3 over these catalysts was carried out with $NO + NH_3$ in 6 : 4 molar ratios. A sharp decrease in NO concentration occurs at 210°C in Pt/CeO_2 and 100% NO conversion occurs below 225°C. Here N_2 and H_2O are the only products. N_2O is not observed. The reaction on M/CeO_2 can be given by

$$6NO + 4NH_3 \rightarrow 5N_2 + 6H_2O. \quad [3]$$

On the other hand, M/Al_2O_3 catalysts give N_2O as a product along with N_2 and H_2O. At higher temperatures N_2O decomposes. The reaction on M/Al_2O_3 catalysts can be written as

$$4NO + 2NH_3 \rightarrow 2N_2 + N_2O + 3H_2O. \quad [4]$$

NO reduction by CH_4. A remarkable low-temperature (350°C) NO reduction by CH_4 occurs over 1% Pt/CeO_2 catalyst giving N_2, CO_2, and H_2O as the products. The corresponding 1% Pd/CeO_2 catalyst shows complete NO conversion at 450°C. The reaction can be written as

$$4NO + CH_4 \rightarrow 2N_2 + CO_2 + 2H_2O. \quad [5]$$

NO reduction by C_3H_8. NO reduction by C_3H_8 over 1% Pt/CeO_2 occurs above 325°C. Mass spectra of NO and C_3H_8 at 25°C and products N_2, H_2O, and CO_2 at 325°C are shown in Figs. 8a and 8b. At 325°C NO is fully utilized by C_3H_8. The reaction can be written as

$$10NO + C_3H_8 \rightarrow 5N_2 + 3CO_2 + 4H_2O. \quad [6]$$

Formation of N_2O ($m/z = 44$) in small quantity cannot be ruled out in the NO reduction by CO, CH_4, and C_3H_8. However, dissociation of N_2O over Pt in the $NO + NH_3$ reaction has been reported by Takoudls and Schmidt (30). Here also even if N_2O is formed it may be dissociated at higher temperature.

CO oxidation by O_2. CO oxidation was carried out over 1% Pt/CeO_2 and 1% Pd/CeO_2 catalysts in the presence of O_2. A sharp decrease in CO concentration is observed at 140°C in the case of 1% Pd/CeO_2 and 100% conversion of CO occurs below 200°C. Similarly, 100% CO conversion occurs at 180°C over 1% Pt/CeO_2. The reaction is written as follows:

$$2CO + O_2 \rightarrow 2CO_2. \quad [7]$$

Hydrocarbon oxidation. Complete CH_4 oxidation occurs over 1% Pt/CeO_2 and 1% Pd/CeO_2 at 390°C and 330°C, respectively, whereas complete oxidation of C_3H_8 over Pt/CeO_2 and Pd/CeO_2 occurs at 110°C and 230°C, respectively. The products are H_2O and CO_2. The reactions can be written as

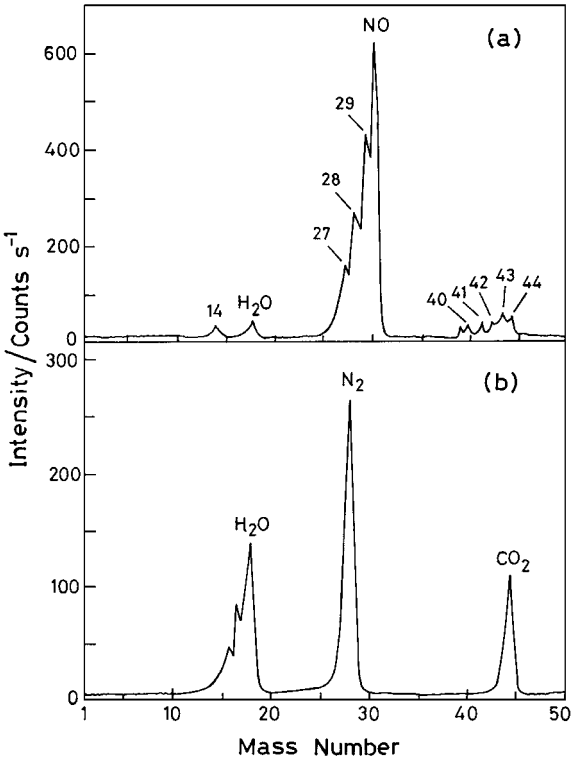

FIG. 8. Mass spectra of $NO + C_3H_8$ reaction over 1% Pt/CeO_2 at (a) 25°C and (b) 325°C.

$$CH_4 + 2O_2 \rightarrow CO_2 + 2H_2O \quad [8]$$

$$C_3H_8 + 5O_2 \rightarrow 3CO_2 + 4H_2O. \quad [9]$$

Temperatures of nearly 100% conversion of NO, CO, CH_4, and C_3H_8 for all the reactions over 1% Pt/CeO_2 and 1% Pd/CeO_2 catalysts are summarized in Table 1. Results on the same reaction over 1% Pt/Al_2O_3 and 1% Pd/Al_2O_3 catalysts are also given in Table 1 for comparison. It may be

TABLE 1

Nearly 100% Conversion Temperatures (°C) of NO, CO, CH_4, and C_3H_8 for the Following Reactions on CeO_2- and Al_2O_3-Supported Pt and Pd Catalysts

Reactions	1% Pt/CeO_2	1% Pt/Al_2O_3	1% Pd/CeO_2	1% Pd/Al_2O_3
$NO + CO$	270	400	175	350
$NO + NH_3$	225	280	275	330
$NO + CH_4$	350	425	450	475
$NO + C_3H_8$	325	475	330	525
$CO + O_2$	180	230	175	230
$CH_4 + O_2$	400	425	330	350
$C_3H_8 + O_2$	110	175	230	300

noted from the table that nearly 100% conversion occurs at a much lower temperature with M/CeO_2 catalysts compared to that with M/Al_2O_3 catalysts for all the reactions. All the reactions over pure CeO_2 occur at much higher temperatures (19).

Temperature-programmed desorption of 1% Pt/CeO_2 and 1% Pd/CeO_2 catalysts was carried out. Oxygen desorption has not been observed up to 550°C. Further, reaction with H_2 over the desorbed catalysts did not show H_2O formation even up to 600°C. This result suggests that O_2 associated with Pt or Pd is strongly bound to the CeO_2 lattice and in NO reduction as well as CO and hydrocarbon oxidation studies it is the feed O_2 which is utilized during the reaction.

Kinetics

The rate of the reactions is calculated by using the equation (31)

$$\text{rate} = \frac{FX}{vW}, \qquad [10]$$

where F is the inlet molar flow rate of the particular gas, X is the fractional conversion of the gas at a particular temperature, v is the stoichiometric coefficient of the gas, and W is the weight of the catalyst. Rate is expressed in micromoles per gram per second. The rates of NO + CO and CO + O_2 are given in Figs. 9 and 10. The turnover frequencies (TOF) of NO and CO conversion at different temperatures have been calculated after dividing the rate (μmol g^{-1} s^{-1}) by the active site concentration (μmol g^{-1}). TOF is expressed in inverse seconds. The active metal site concentration has been obtained from the amount of the metal present in 1 g of the catalyst. For example, 5.74×10^{-5} mol of Pt is present in 1 g of 1% Pt/CeO_2 catalyst. The rate and TOF data of NO + CO and CO + O_2 reactions over Pt/CeO_2 and Pd/CeO_2 catalysts are summarized in Table 2. TOF values are higher for M/CeO_2 catalysts compared to those for M/Al_2O_3 catalysts. TOF of CO oxidation on combustion-synthesized Pd/Al_2O_3 is higher than that of the same reaction on same catalyst prepared by the incipient wetness method (32, 33).

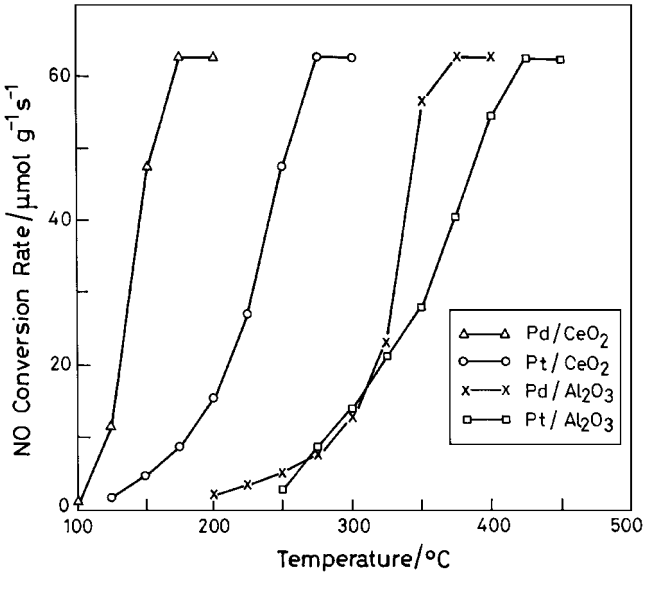

FIG. 9. Rate of NO conversion over CeO_2- and Al_2O_3-based catalysts for NO + CO reaction.

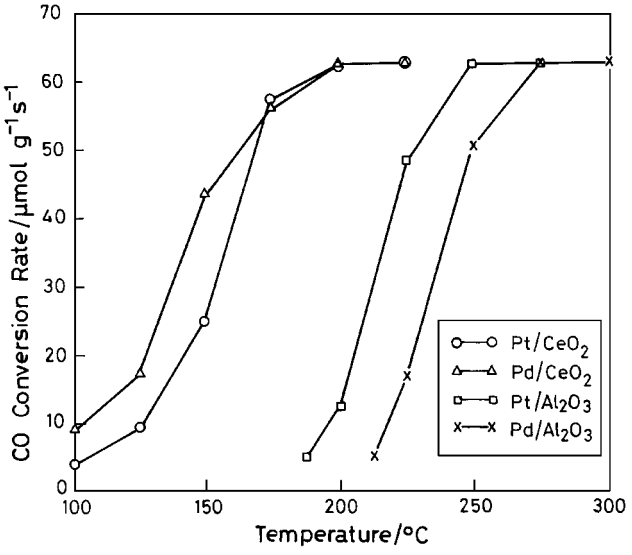

FIG. 10. Rate of CO conversion over CeO_2- and Al_2O_3-based catalysts for CO + O_2 reaction.

The activation energy (E_a) has been calculated from Arrhenius plots of ln(rate) vs $1/T$ for NO + CO and CO + O_2 reactions over these catalysts. Here, CO_2 formation rates were taken into account to calculate the activation energy. There is a remarkable difference in activation energy between CeO_2- and Al_2O_3-supported Pt and Pd catalysts. For CO + O_2 reaction over Pt/CeO_2 E_a is 31.2 kJ mol^{-1} whereas that for Pt/Al_2O_3 is 53.9 kJ mol^{-1}. Similarly, for NO + CO reaction over Pd/CeO_2 and Pd/Al_2O_3 E_a are

TABLE 2

Rate (μmol g^{-1} s^{-1}) and TOF (s^{-1}) Data of NO + CO and CO + O_2 Reactions over CeO_2- and Al_2O_3-Supported Pt and Pd Catalysts

	NO + CO		CO + O_2	
Catalysts	Rate	TOF	Rate	TOF
1% Pt/CeO_2	27.10 (225°C)	0.47 (225°C)	25.00 (150°C)	0.44 (150°C)
	47.50 (250°C)	0.83 (250°C)	57.08 (175°C)	0.99 (175°C)
1% Pd/CeO_2	11.88 (125°C)	0.21 (125°C)	43.75 (150°C)	0.76 (150°C)
	47.50 (150°C)	0.82 (150°C)	56.67 (175°C)	0.98 (175°C)
1% Pt/Al_2O_3	40.42 (375°C)	0.42 (375°C)	12.92 (200°C)	0.13 (200°C)
	54.58 (400°C)	0.57 (400°C)	48.33 (225°C)	0.50 (225°C)
1% Pd/Al_2O_3	23.31 (325°C)	0.24 (325°C)	17.10 (225°C)	0.18 (225°C)
	56.25 (350°C)	0.58 (350°C)	50.83 (250°C)	0.52 (250°C)

52.6 and 60.6 kJ mol^{-1}, respectively. Activation energies of CO oxidation on Pd/Al_2O_3, Pt/Al_2O_3 and Pt/CeO_2 are lower than the values reported in the literature (33–36).

DISCUSSIONS

The combustion method involves rapid heating of an aqueous solution containing stoichiometric amounts of corresponding metal nitrates and hydrazine-based fuels. During the combustion the temperature reached for a short period (1–2 min) is about 1000°C. Evolution of a large amount of gases during the process is responsible for fine crystallite formation. So in combustion-derived M/CeO_2, Pt or Pd ions should either be separated into Pt or Pd metal clusters (as in Pt/Al_2O_3) or Pt, Pd oxide clusters separated from oxide support or ions should be incorporated. In the case of Pt/CeO_2 and Pd/CeO_2, Pt and Pd ions seem to be incorporated due to low metal loading (1% by mole). Solid solution of the type $Ce_{1-x}M_xO_{2-x}$ is one of the routes of incorporation of ions in CeO_2. In contrast to this, in the impregnation method for example, Pt^{2+}, Pd^{2+} ions in solution are dispersed on already prepared CeO_2 substrate and dried at relatively low temperature (<500°C). Thus, some of the important merits of the combustion method are fine crystallites formation, easy incorporation of dopant ions in the support/host lattice, no need of a hydrogen reduction step, and purity of the catalysts.

In the present study all the catalytic reactions were carried out over as-prepared 1% Pt/CeO_2 and 1% Pd/CeO_2 samples and therefore, investigation of chemical states of Pt or Pd in these samples is important. It is clear from the XRD as well as TEM studies that neither the metal particles nor any of the oxide phases of Pt or Pd on CeO_2 are observed in 1% Pt/CeO_2 and 1% Pd/CeO_2. XPS studies show that Pt is in the +2 and +4 and Pd is in the +2 oxidation states in 1% Pt/CeO_2 and 1% Pd/CeO_2, respectively. Even in 10% Pd/CeO_2, Pd(3*d*) peaks observed from XPS correspond to the Pd^{2+} state. These observations suggest that Pt and Pd ions are incorporated in CeO_2 in the form of a solid solution, $Ce_{1-x}M_xO_{2-(4-n)x/2}$. The ionic radii (37) of Pt^{2+} (80 pm) and Pd^{2+} (86 pm) are closer to that of Ce^{4+} (97 pm). Therefore, if these metal ions are formed in the preparation condition, Pt^{2+}, Pd^{2+} ions can form solid solution of the type $Ce_{1-x}M_xO_{2-x}$ ($M = Pt^{2+}$, Pd^{2+}).

By the combustion method Pt and Pd ions are homogeneously dispersed on nanosize CeO_2 crystallites in a single step. Considering a 15-nm mean size of CeO_2 crystallites, the Ce^{4+} ion concentration on the crystallite surfaces can be calculated from its lattice parameter *a*. Assuming that Pt ions are ionically dispersed on the CeO_2 surface we find that 20% Ce^{4+} ions can be replaced by Pt ions in 1% Pt/CeO_2. Observations of Pt in the +2 and +4 states and 15% surface concentration of Pt from XPS studies (against 1% taken in the preparation) suggest that almost all the Pt ions are ionically dispersed on the CeO_2 crystallite surface. Unlike the case of Pt/CeO_2, the surface concentration of Pd is only 5% for 1% Pd/CeO_2. Pd^{2+} in Pd/CeO_2 is highly ionic in nature. Further, Pd^{2+} is a more stable ion. Therefore, it is possible that Pd^{2+} ion can form solid solution $Ce_{1-x}Pd_xO_{2-x}$ indicating that all the Pd metal taken in the preparation may not be dispersed on the CeO_2 crystallite surface. This is further supported by the fact that even up to 10% Pd/CeO_2 could be prepared without any PdO or Pd metal formation by the combustion method. From these studies we propose the presence of $-O^{2-}-Ce^{4+}-O^{2-}-M^{n+}-O^{2-}-$ type of linkages on the CeO_2 surface. Oxygen ion vacancies are created due to lower valent ionic substitution for Ce^{4+} ions. Oxygen ion vacancy should have beneficial effects on catalytic activities due to the increase in oxygen ion mobility.

All the reactions over CeO_2-supported Pt and Pd catalysts occur at much lower temperature compared to those over Al_2O_3-supported Pt and Pd catalysts (Table 1). But CeO_2-promoted Pd/Al_2O_3 is shown to suppress the alkane oxidation (38–40). In these studies, addition of CeO_2 to Pd/Al_2O_3 enhances PdO formation in the presence of O_2 along with $CeAlO_3$ phase formation. In Pd/CeO_2 catalysts prepared here, formation of a PdO phase has not been observed. The higher activity of the Pd/CeO_2 catalyst noticed here may be due to the availability of dissociated oxygen via oxide ion defects formed in $Ce_{1-x}Pd_xO_{2-x}$. In general, the reasons for the drastic decrease in reaction temperature over M/CeO_2 compared to M/Al_2O_3 can be attributed to a strong metal–ceria interaction. Ionic dispersion of Pt and Pd metals in the form of a solid solution brings about metal ion incorporation in the CeO_2 matrix. Since only 1% of Ce^{4+} ions are substituted by Pt^{2+} or Pd^{2+} ions, O^{2-} ions associated with the metal ions are bonded to Ce^{4+} ions. This seems to be the reason for the stability of Pt^{2+} and Pd^{2+} ions toward reduction. As pure CeO_2 does not show CO adsorption or any of the catalytic reactions at such low temperatures, therefore, the active adsorption sites for NO, CO, NH_3, and other gases have to be Pt^{2+} and Pd^{2+} ions on CeO_2 surface. A nearly 10 times increase in CO adsorption per mole of Pt in 1% Pt/CeO_2 compared to 1% Pt/Al_2O_3 is due to the higher dispersion of Pt on the CeO_2 surface. Accordingly, CO oxidation and NO reduction rates and TOFs are higher on Pt/CeO_2 compared to those on Pt/Al_2O_3.

Electronic interaction involving $Ce^{4+}(4f)$, $O^{2-}(2p)$, and $Pd^{2+}(4d)$ or $Pt^{2+}(5d)$ orbitals may facilitate the redox reactions. For example, in the $NO + NH_3$ redox reaction, electrons released from NH_3 may be transferred to NO via $-M^{2+}-O^{2-}-Ce^{4+}-M^{2+}-$ linkages leading to redox exchange:

$$-Ce^{4+}-O^{2-}-M^{2+}- + e \Leftrightarrow -Ce^{4+}-O^{2-}-M^{+}-$$
$$\Leftrightarrow -Ce^{3+}-O^{2-}-M^{2+}- \Leftrightarrow -Ce^{4+}-O^{2-}-M^{2+}- + e.$$

In any case, such a possibility does not exist in M/Al_2O_3 catalysts. Therefore, the metal–ceria interaction appears to play

an important role in lowering the reaction temperature. Detailed mechanism of these reactions involving Pt and Pd ions over CeO_2 needs further investigations.

CONCLUSIONS

In conclusion, we have shown a new process of dispersing Pt and Pd in the ionic form on a CeO_2 surface by the combustion method. Characterization techniques employed here are XRD, TEM, and XPS. Catalytic activities for NO reduction and CO and hydrocarbon oxidation over these catalysts have been examined by TPR. The salient features of our studies are the following.

(1) Pt and Pd ions dispersed over CeO_2 crystallites of 15–20 nm have been synthesized by the combustion technique.

(2) Pt is in the +2 and +4 states in 1% Pt/CeO_2 and Pd is found to be in the +2 state in 1% Pd/CeO_2.

(3) There is a metal–ceria interaction which leads to the formation of a solid solution, $Ce_{1-x}M_xO_{2-(4-n)x/2}$.

(4) Active adsorption sites for the catalytic reactions are noble metal ions in M/CeO_2 catalysts.

(5) NO reduction and CO and hydrocarbon oxidation temperatures are much lower over M/CeO_2 catalysts compared to those over M/Al_2O_3 catalysts.

(6) M/CeO_2 catalysts show higher rates and TOFs for $NO + CO$ and $CO + O_2$ reactions.

ACKNOWLEDGMENTS

P.B. and K.C.P. thank the Council of Scientific and Industrial Research (CSIR), Govt. of India, for financial support. The Department of Atomic Energy (DAE), Govt. of India, is gratefully acknowledged for funding this research.

REFERENCES

1. Howitt, C., Pitchon, V., and Maire, G., *J. Catal.* **154**, 47 (1995).
2. Taylor, K. C., *Catal. Rev.-Sci. Eng.* **35**, 457 (1993).
3. Yao, H. C., and Yao, Y.-F. Y., *J. Catal.* **86**, 254 (1984).
4. Kummer, J. T., *J. Phys. Chem.* **90**, 4747 (1986).
5. Oh, S. H., *J. Catal.* **124**, 477 (1990).
6. Oh, S. H., and Eickel, C. C., *J. Catal.* **112**, 543 (1988).
7. Lööf, B., Kasemo, B., and Keck, K.-E., *J. Catal.* **118**, 339 (1989).
8. Thomas, J. M., and Thomas, W. J., "Principles and Practice of Heterogeneous Catalysis," p. 577. VCH, Weinheim, 1997.
9. Fernández-García, M., Martínez-Arias, A., Salamanca, L. N., Coronado, J. M., Anderson, J. A., Conesa, J. C., and Soria, J., *J. Catal.* **187**, 474 (1999).
10. Summers, J. C., and Ausen, S. A., *J. Catal.* **58**, 131 (1979).
11. Jin, T., Okuhara, T., Mains, G. J., and White, J. M., *J. Phys. Chem.* **91**, 3310 (1987).
12. Jin, T., Zhou, Y., Mains, G. J., and White, J. M., *J. Phys. Chem.* **91**, 5931 (1987).
13. Harrison, B., Diwell, A. F., and Hallett, C., *Platinum Metals Rev.* **32**, 73 (1988).
14. Lööf, P., Kasemo, B., Andersson, S., and Frestad, A., *J. Catal.* **130**, 181 (1991).
15. Nunan, J. G., Robota, H. J., Cohn, M. J., and Bradley, S. A., *J. Catal.* **133**, 309 (1992).
16. Serre, C., Garin, F., Belot, G., and Maire, G., *J. Catal.* **141**, 1 (1993).
17. Serre, C., Garin, F., Belot, G., and Maire, G., *J. Catal.* **141**, 9 (1993).
18. Martínez-Arias, A., Coronado, J. M., Cataluña, R., Conesa, J. C., and Soria, J., *J. Phys. Chem. B* **102**, 4357 (1998).
19. Bera, P., Aruna, S. T., Patil, K. C., and Hegde, M. S., *J. Catal.* **186**, 36 (1999).
20. Bera, P., Patil, K. C., Jayaram, V., Hegde, M. S., and Subbanna, G. N., *J. Mater. Chem.* **9**, 1801 (1999).
21. Bera, P., Patil, K. C., and Hegde, M. S., *Phys. Chem. Chem. Phys.* **2**, 373 (2000).
22. Graw, G., *Anal. Chim. Acta* **14**, 150 (1956).
23. Hegde, M. S., Ramesh, S., and Ramesh, G., *Proc. Indian Acad. Sci. Chem. Sci.* **104**, 591 (1992).
24. Shyu, J. Z., and Otto, K., *J. Catal.* **115**, 16 (1989).
25. Briggs, D., and Seah, M. P., "Practical Surface Analysis by Auger and X-ray Photoelectron Spectroscopy," Appendix 4. Wiley, New York, 1984.
26. Sarma, D. D., Hegde, M. S., and Rao, C. N. R., *J. Chem. Soc., Faraday Trans. 2* **77**, 1509 (1981).
27. Scofield, J. H., *J. Electron Spectrosc. Relat. Phenom.* **8**, 129 (1976).
28. Penn, D. R., *J. Electron Spectrosc. Relat. Phenom.* **29**, 9 (1976).
29. Gruber, H. L., *J. Phys. Chem.* **66**, 48 (1962).
30. Takoudls, C. G., and Schmidt, L. D., *J. Phys. Chem.* **87**, 958 (1983).
31. Burwell, R. L., Jr., *Pure Appl. Chem.* **46**, 71 (1976).
32. Choi, K. I., and Vannice, M. A., *J. Catal.* **131**, 1 (1991).
33. Rainer, D. R., Koranne, M., Vesecky, S. M., and Goodman, D. W., *J. Phys. Chem. B* **101**, 10769 (1997).
34. Yao, Y.-F. Y., *J. Catal.* **87**, 152 (1984).
35. Cant, N. W., Hicks, P. C., and Lennon, B. S., *J. Catal.* **54**, 372 (1978).
36. Hardacre, C., Ormerod, R. M., and Lambert, R. M., *J. Phys. Chem.* **98**, 10901 (1994).
37. Shannon, R. D., *Acta Crystallogr. A* **32**, 751 (1976).
38. Yao, Y.-F. Y., *Ind. Eng. Chem. Prod. Res. Dev.* **19**, 293 (1980).
39. Shyu, J. Z., Otto, K., Watkins, W. L. H., Graham, G. W., Belitz, R. K., and Gandhi, H. S., *J. Catal.* **114**, 23 (1988).
40. Oh, S. H., Mitchell, P. J., and Siewert, R. M., *J. Catal.* **132**, 287 (1991).